A QUADRATIC FINITE ELEMENT WAVELET RIESZ BASIS

NIKOLAOS REKATSINAS AND ROB STEVENSON

Abstract. In this paper, continuous piecewise quadratic finite element wavelets are constructed on general polygons in $\mathbb{R}^2$. The wavelets are stable in H^s for $|s| < \frac{3}{2}$ and have two vanishing moments. Each wavelet is a linear combination of 11 or 13 nodal basis functions. Numerically computed condition numbers for $s \in \{-1, 0, 1\}$ are provided for the unit square.

1. Introduction

It is well-known that, properly scaled, an infinite countable collection of wavelets can generate Riesz bases for a scale of Sobolev spaces. Such wavelets can be applied for the numerical solution of PDEs and singular integral equations. For suitable wavelets, the (infinite) stiffness matrix of such an operator equation is boundedly invertible, so that the residual of an approximation is equivalent to its error, meaning that this residual can be used as an a posteriori error estimator for driving an adaptive algorithm. Using that wavelets have vanishing moments, even for singular integral equations the matrix is close to being sparse, and therefore its application can be efficiently approximated. Furthermore, in any case for elliptic equations, any principal submatrix is uniformly well-conditioned allowing for an efficient iterative solution of the arising Galerkin systems.

As with most wavelet applications, it is important that the wavelets have local supports. Other than with classical wavelet applications, as data compression and signal analysis, for solving operator equations the corresponding dual wavelets do not enter the computations, and their support sizes are irrelevant. This induces a lot of freedom in the construction of suitable wavelet bases. For more information on the application of wavelets for the (adaptive) solution of operator equations, we refer to [Dah97, Ste09, Urb09] and the references cited there.

Traditionally, wavelets are constructed on the line or on the interval $[0, 1]$. Then the application of a tensor product construction yields wavelets on $\mathbb{R}^n$ or $[0, 1]^n$. For equipping more general domains in $\mathbb{R}^n$, or their boundaries, with wavelet bases, domain decomposition techniques have been developed (e.g. [CTU99, DS99a, DS99b]).

Another approach to treat non-product domains is to construct wavelets in finite element spaces w.r.t. a nested sequence of meshes. This approach, to which also this paper is devoted, inherits the full flexibility from the finite element method concerning the shape of the domain.

Date: February 12, 2018.

2010 *Mathematics Subject Classification.* 65T60, 65N30 41A10, 42C40.

Key words and phrases. Wavelets, finite elements, Riesz bases, biorthogonality, vanishing moments.

The first author has been supported by the Netherlands Organization for Scientific Research (NWO) under contract. no. 613.001.216.

To realize the Riesz basis property, one can rely on the theory of biorthogonal space decompositions ([Dah96]). It starts with two multiresolution analyses $(V_j)_{j\geq 0}$, $(\tilde{V}_j)_{j\geq 0}$ on the given domain that both satisfy Jackson and Bernstein estimates, and for which V_j and $\tilde{V}_j$ are relatively close in the sense that they satisfy inf-sup conditions, uniformly in j. Then for each j, one constructs the wavelets on 'level' j as a uniformly L_2 well-conditioned basis for the biorthogonal complement $V_j \cap \tilde{V}_{j-1}^{\perp_{L_2}}$ of V_{j-1} in V_j. The union over j of such wavelets form, properly scaled, a Riesz basis for the Sobolev space with smoothness index s for s in an interval $(s_{\min}, s_{\max}) \ni 0$ determined by the aforementioned Jackson and Bernstein estimates. With finite element wavelets, both multiresolution analyses are sequences of finite element spaces w.r.t. a common sequence of meshes. Linear finite elements of this type, with $\tilde{V}_j = V_j$, were constructed in [KO95, Ste98a, FQ00, HM00], and higher order ones, also with $\tilde{V}_j \neq V_j$, can be found in [DS99c, NS09]. With the exception of [Ste98a], the constructions in these references were restricted to two space dimensions.

An alternative possibility is to relax 'true' biorthogonality w.r.t. L_2 to an approximate biorthogonality, for instance biorthogonality w.r.t. to a level-dependent, approximate L_2-scalar product. Usually the resulting wavelet bases have smaller supports than those than span truly L_2-biorthogonal complements, but on the other hand typically their $s_{\min}$ is larger and sometimes positive. Linear finite element wavelets of this type can be found in [VW96, Ste98b, LO96], and quadratic ones in [Liu06].

In [RS18], we applied an adaptive wavelet method for solving time-dependent parabolic PDEs in a simultaneous space-time variational formulation. One of the arising spaces that had to be equipped with a wavelet Riesz basis is the intersection of the Bochner spaces $L_2((0,T); H_0^1(\Omega)) \cap H^1((0,T); H^{-1}(\Omega))$, where $\Omega \subset \mathbb{R}^2$ denotes the spatial domain. We equipped this space with a basis of tensor products of temporal wavelets and spatial wavelets. In order to obtain a Riesz basis for the aforementioned intersection space, the collection of temporal wavelets has to be, properly scaled, a Riesz basis for $L_2(0,T)$ and for $H^1(0,T)$, which collections of wavelets are amply available, whereas the collection Ψ of spatial wavelets has to be, properly scaled, a Riesz basis for $H_0^1(\Omega)$ and for its dual $H^{-1}(\Omega)$. Moreover, in order to obtain a sufficient near-sparsity of the resulting stiffness matrix, we need these wavelets from Ψ to have 2 vanishing moments, or more precisely, cancellation properties of order 2. Finally, since we wrote the PDE as a first order system least squares system, and a suitable wavelet basis for the flux variable is at least of order 2, we need the wavelets from Ψ to be of order 3, i.e. piecewise quadratics.

Piecewise quadratic wavelets in finite element spaces were constructed in [DS99c, Liu06, NS09]. Those in [Liu06] have small supports, but are not stable in H^s for $s \leq 0$ and do not have vanishing moments. The quadratic wavelets in the other two references satisfy our needs, and have even 3 vanishing moments ($\tilde{V}_j = V_j$). Unfortunately the condition numbers of those from [DS99c] turned out to be very large. For that reason, in [NS09] we applied the available freedom in the general construction from [DS99c] to arrive at wavelets that are much better conditioned. The price to be paid was an increased support size. The continuous piecewise quadratic finite element wavelets from [NS09] are linear combinations of 87 nodal basis functions. In the current work, we change $\tilde{V}_j$ into the space of continuous piecewise linears w.r.t. a dyadically refined mesh, and use the fact that the latter space can be equipped with basis functions of smaller supports to construct piecewise quadratic wavelets that satisfy all our needs, have condition numbers similar to those from [NS09], and are given as linear combinations of 11 or 13 nodal basis functions (these numbers depend on the valence of the vertices in the initial mesh, and the current numbers apply when this valence is 6). The same construction principle can be applied in three dimensions, but it will require calculations on a reference tetrahedron that so far we have not performed.

This paper is organized as follows: In Sect. 2 we review the general theory on biorthogonal space decompositions, and in Sect. 3 we apply the general principles of the element-by-element construction of finite element wavelets to construct continuous piecewise quadratic wavelets in two space dimensions, with small supports and 2 vanishing moments. We provide numerically computed condition numbers in H^1, L_2 and H^{-1}-norms.

We will use the following notations. By $C \lesssim D$ we will mean that C can be bounded by a multiple of D, independently of parameters which C and D may depend on. Obviously, $C \gtrsim D$ is defined as $D \lesssim C$, and $C \eqsim D$ as $C \lesssim D$ and $C \gtrsim D$.

For normed linear spaces $\mathscr{A}$ and $\mathscr{B}$, for convenience in this paper always over $\mathbb{R}$, $\mathcal{L}(\mathscr{A},\mathscr{B})$ will denote the space of bounded linear mappings $\mathscr{A} \to \mathscr{B}$ endowed with the operator norm $\|\cdot\|_{\mathcal{L}(\mathscr{A},\mathscr{B})}$.

For a countable set $\vee$, the norm and scalar product on $\ell_2(\vee)$ will be denoted as $\|\cdot\|$ and $\langle\,,\,\rangle$, respectively. For real square matrices A and B of the same size, we write $A \geq B$ when for all real vectors x, $\langle Ax, x\rangle \geq \langle Bx, x\rangle$.

A countable collection of functions Σ will be formally viewed as a column vector. Then for a sequence of scalars $\mathbf{c} = (c_\sigma)_{\sigma\in\Sigma}$, we set $\mathbf{c}^\top\Sigma := \sum_{\sigma\in\Sigma} c_\sigma \sigma$. For countable collections of functions Σ and Φ in a Hilbert space $\mathscr{H}$, we define the (formal) matrix $\langle \Sigma, \Phi\rangle_{\mathscr{H}} := [\langle \sigma, \phi\rangle_{\mathscr{H}}]_{\sigma\in\Sigma,\phi\in\Phi}$.

We use the symbol $\mathbb{N}_0$ to denote $\{0, 1, \cdots\}$.

2. Theory on biorthogonal wavelet bases

Let $\mathscr{V}, \tilde{\mathscr{V}}, \mathscr{H}$ be separable Hilbert spaces with $\mathscr{V}, \tilde{\mathscr{V}} \hookrightarrow \mathscr{H}$ with dense embedding. Identifying $\mathscr{H}$ with its dual, we obtain the Gelfand triples $\mathscr{V} \hookrightarrow \mathscr{H} \hookrightarrow \mathscr{V}'$ and $\tilde{\mathscr{V}} \hookrightarrow \mathscr{H} \hookrightarrow \tilde{\mathscr{V}}'$ with dense embeddings. For $s \in [-1, 1]$, we set the interpolation spaces $\mathscr{V}^s := [\mathscr{V}', \mathscr{V}]_{\frac{1}{2}s+\frac{1}{2}}$ and $\tilde{\mathscr{V}}^s := [\tilde{\mathscr{V}}', \tilde{\mathscr{V}}]_{\frac{1}{2}s+\frac{1}{2}}$. The following theorem is a special case of an even more general result proven in [Dah96].

Theorem 2.1 (Biorthogonal space decompositions, [DS99c])**.** *Consider two* multiresolution analyses

$$V_0 \subset V_1 \subset \cdots \subset \mathscr{H}, \text{ with } \operatorname{clos}_{\mathscr{H}}(\cup_{j\geq 0} V_j) = \mathscr{H},$$
$$\tilde{V}_0 \subset \tilde{V}_1 \subset \cdots \subset \mathscr{H}, \text{ with } \operatorname{clos}_{\mathscr{H}}(\cup_{j\geq 0} \tilde{V}_j) = \mathscr{H}.$$

Suppose that for $j \geq 0$ there exist uniformly bounded biorthogonal projectors $Q_j \in \mathcal{L}(\mathscr{H},\mathscr{H})$ such that

$$\operatorname{ran} Q_j = V_j, \quad \operatorname{ran}(I - Q_j) = \tilde{V}_j^{\perp_{\mathscr{H}}}, \tag{2.1}$$

and, for some $\rho,\, \tilde\rho > 1$,

$$\begin{aligned} &\inf_{v_j\in V_j} \|v-v_j\|_{\mathscr H} \lesssim \rho^{-j}\|v\|_{\mathscr V} \quad (v\in\mathscr V),\\ &\inf_{\tilde v_j\in \tilde V_j} \|\tilde v-\tilde v_j\|_{\mathscr H} \lesssim \tilde\rho^{-j}\|\tilde v\|_{\tilde{\mathscr V}} \quad (\tilde v\in\tilde{\mathscr V}),\end{aligned} \tag{2.2}$$

and

$$\|v_j\|_{\mathscr V} \lesssim \rho^j\|v_j\|_{\mathscr H} \quad (v_j\in V_j),\quad \|\tilde v_j\|_{\tilde{\mathscr V}} \lesssim \tilde\rho^j\|\tilde v_j\|_{\mathscr H} \quad (\tilde v\in \tilde V_j). \tag{2.3}$$

Then, with $Q_{-1}:=0$*, for every* $s\in(-1,1)$ *it holds that*

$$\|v\|^2_{\mathscr V^s} \eqsim \sum_{j=0}^\infty \rho^{2js}\|(Q_j-Q_{j-1})v\|^2_{\mathscr H} \quad (v\in\mathscr V^s).$$

Remark 2.2 (e.g. [Ste03]). Existence of the biorthogonal projector Q_j as in (2.1) is equivalent to each of the following conditions:

1. (1) $\beta_j := \inf_{0\neq v_j\in V_j}\sup_{0\neq\tilde v_j\in\tilde V_j} \frac{\langle v_j,\tilde v_j\rangle_{\mathscr H}}{\|v_j\|_{\mathscr H}\|\tilde v_j\|_{\mathscr H}} = \inf_{0\neq\tilde v_j\in\tilde V_j}\sup_{0\neq v_j\in V_j} \frac{\langle v_j,\tilde v_j\rangle_{\mathscr H}}{\|v_j\|_{\mathscr H}\|\tilde v_j\|_{\mathscr H}} > 0,$
2. (2) for any Riesz basis Φ_j for V_j there exists a (unique) $\mathscr H$-dual Riesz basis $\tilde\Phi_j$ for $\tilde V_j$,
3. (3) there exist some Riesz bases Φ_j and $\tilde\Phi_j$ for V_j and $\tilde V_j$, respectively, such that $\langle\Phi_j,\tilde\Phi_j\rangle_{\mathscr H}$ is bounded invertible.

It holds that $\|Q_j\|^{-1}_{\mathcal L(\mathscr H,\mathscr H)} = \beta_j \geq \frac{\|\langle\Phi_j,\tilde\Phi_j\rangle^{-1}_{\mathscr H}\|^{-1}}{\sqrt{\|\langle\Phi_j,\Phi_j\rangle_{\mathscr H}\|\|\langle\tilde\Phi_j,\tilde\Phi_j\rangle_{\mathscr H}\|}}$.

Corollary 2.3. *In the situation of Thm. 2.1, for* $j\geq 0$ *let* $\Psi_j=\{\psi_{j,x}\colon x\in J_j\}$ *be a* uniform *Riesz basis for* $\operatorname{ran}(Q_j-Q_{j-1}) = V_j\cap \tilde V_{j-1}^{\perp_{\mathscr H}}$ $(\tilde V_{-1}:=\{0\})$*, i.e., with* $\kappa_{\mathscr H}(\Psi_j) := \|\langle\Psi_j,\Psi_j\rangle_{\mathscr H}\|\|\langle\Psi_j,\Psi_j\rangle^{-1}_{\mathscr H}\|$ *it holds that* $\sup_j\kappa_{\mathscr H}(\Psi_j)<\infty$*. Then for* $s\in(-1,1)$*,*

$$\bigcup_{j=0}^\infty \rho^{-js}\Psi_j \text{ is a Riesz basis for } \mathscr V^s.$$

In particular, with κ_s *denoting the quotient of the supremum and infimum over* $v\in\mathscr V_s$ *of* $\|v\|^2_{\mathscr V^s}/\sum_{j=0}^\infty\rho^{2js}\|(Q_j-Q_{j-1})v\|^2_{\mathscr H}$ *, it holds that*

$$\kappa_{\mathscr V^s}\Big(\bigcup_{j=0}^\infty\rho^{-js}\Psi_j\Big) \leq \kappa_s\times\sup_{j\geq 0}\kappa_{\mathscr H}(\Psi_j).$$

Recalling that $\operatorname{ran}(Q_0-Q_{-1}) = V_0$, the remaining challenge is the construction of Ψ_j for $j\geq 1$, i.e. Ψ_{j+1} for $j\geq 0$:

Proposition 2.4 ([NS09])**.** *For* $j\geq 0$*, let* $\Theta_j\cup\Sigma_{j+1}$ *and* $\tilde\Phi_j$ *be uniform Riesz bases for* V_{j+1} *and* $\tilde V_j$*, respectively, such that* $\langle\Theta_j,\tilde\Phi_j\rangle_{\mathscr H}=\mathrm{Id}$*. Then*

$$\Psi_{j+1} = \Xi_{j+1} - \langle\Xi_{j+1},\tilde\Phi_j\rangle_{\mathscr H}\Theta_j \tag{2.4}$$

is a uniform Riesz basis for $V_{j+1}\cap\tilde V_j^{\perp_{\mathscr H}} = \operatorname{ran}(Q_{j+1}-Q_j)$*.*

With

$$\delta_j := \inf_{0\neq \hat{v}_j \in \operatorname{span}\Theta_j} \sup_{0\neq \tilde{v}_j \in \tilde{V}_j} \frac{\langle \hat{v}_j, \tilde{v}_j\rangle_{\mathscr{H}}}{\|\hat{v}_j\|_{\mathscr{H}}\|\tilde{v}_j\|_{\mathscr{H}}},$$

$$\varepsilon_j := \sup_{0\neq \hat{v}_j \in \operatorname{span}\Theta_j} \sup_{0\neq w_{j+1} \in \operatorname{span}\Xi_{j+1}} \frac{\langle \hat{v}_j, w_{j+1}\rangle_{\mathscr{H}}}{\|\hat{v}_j\|_{\mathscr{H}}\|w_{j+1}\|_{\mathscr{H}}},$$

it holds that

$$\kappa_{\mathscr{H}}(\Psi_{j+1}) \leq \frac{(1+\delta_j^{-1})}{\sqrt{1-\varepsilon_j}}\kappa_{\mathscr{H}}(\Xi_{j+1}).$$

To complete our overview of the theory of biorthogonal space decompositions and wavelets, in the next two remarks we discuss dual wavelets. The first remark will become relevant for the numerical approximation of the $H^{-1}(\Omega)$-condition numbers of the (primal) wavelets that we will construct. The second remark will shed light on the difference between the general setting of biorthogonal space decompositions that we consider, and the more restricted framework for the construction of locally supported wavelets, whose duals are locally supported too, that is usually considered in one dimension.

Remark 2.5 (dual wavelets). With $(\,)^*$ denoting the adjoint w.r.t. $\langle\,,\,\rangle_{\mathscr{H}}$, under the conditions of Thm 2.1 equivalently it holds that for every $s \in (-1,1)$,

$$\|\tilde{v}\|^2_{\tilde{\mathscr{V}}^s} \eqsim \sum_{j=0}^{\infty} \rho^{2js}\|(Q_j^* - Q_{j-1}^*)\tilde{v}\|^2_{\mathscr{H}} \quad (\tilde{v} \in \tilde{\mathscr{V}}^s),$$

so that for $\tilde{\Psi}_j$ being *any* uniform Riesz basis for $\operatorname{ran}(Q_j^* - Q_{j-1}^*) = \tilde{V}_{j+1} \cap V_j^{\perp_{\mathscr{H}}}$,

$$\bigcup_{j=0}^{\infty} \rho^{-js}\tilde{\Psi}_j \text{ is a Riesz basis for } \tilde{\mathscr{V}}^s.$$

One verifies that the pair $(\operatorname{ran}(Q_j^* - Q_{j-1}^*), \operatorname{ran}(Q_j - Q_{j-1}))$ satisfies (1) with infsup constant $\gamma_j := \|Q_j - Q_{j-1}\|^{-1}_{\mathcal{L}(\mathscr{H},\mathscr{H})} \gtrsim 1$. Consequently, as stated in Remark 2.2, given a Riesz basis Ψ_j for $\operatorname{ran}(Q_j - Q_{j-1})$, there exists a unique dual or biorthogonal Riesz basis $\tilde{\Psi}_j$ for $\operatorname{ran}(Q_j^* - Q_{j-1}^*)$, i.e. with $\langle \Psi_j, \tilde{\Psi}_j\rangle_{\mathscr{H}} = \mathrm{Id}$. From

$$\gamma_j \|\mathbf{c}_j^\top \tilde{\Psi}_j\|_{\mathscr{H}} \leq \sup_{0\neq v_j \in \operatorname{ran}(Q_j - Q_{j-1})} \frac{\langle \mathbf{c}_j^\top \tilde{\Psi}_j, v_j\rangle_{\mathscr{H}}}{\|v_j\|_{\mathscr{H}}} \leq \|\mathbf{c}_j^\top \tilde{\Psi}_j\|_{\mathscr{H}},$$

and

$$\sup_{0\neq v_j \in \operatorname{ran}(Q_j - Q_{j-1})} \frac{\langle \mathbf{c}_j^\top \tilde{\Psi}_j, v_j\rangle_{\mathscr{H}}}{\|v_j\|_{\mathscr{H}}} = \sup_{0\neq \mathbf{d}_j} \frac{\langle \mathbf{c}_j^\top \tilde{\Psi}_j, \mathbf{d}_j^\top \Psi_j\rangle_{\mathscr{H}}}{\|v_j\|_{\mathscr{H}}} = \sup_{0\neq \mathbf{d}_j} \frac{\langle \mathbf{c}_j, \mathbf{d}_j\rangle}{\|\mathbf{d}_j\|} \frac{\|\mathbf{d}_j\|}{\|\mathbf{d}_j^\top \Psi_j\|_{\mathscr{H}}}$$

one infers that $\kappa_{\mathscr{H}}(\tilde{\Psi}_j) \leq \gamma_j^{-1}\kappa_{\mathscr{H}}(\Psi_j)$. Consequently, when the Ψ_j are uniform Riesz bases for $\operatorname{ran}(Q_j - Q_{j-1})$, then their duals are uniform Riesz bases for $\operatorname{ran}(Q_j^* - Q_{j-1}^*)$, and for $s \in (-1,1)$, $\bigcup_{j=0}^\infty \rho^{-js}\Psi_j$ and $\bigcup_{j=0}^\infty \rho^{js}\tilde{\Psi}_j$ are $\mathscr{H}$-biorthogonal Riesz bases for $\mathscr{V}^s$ and $\tilde{\mathscr{V}}^{-s}$, respectively.

Moreover, if $\tilde{\mathscr{V}} = \mathscr{V}$, then from $\|\mathbf{c}^\top \mathbf{D}\Psi\|_{\mathscr{V}^s} = \sup_{0\neq \mathbf{d} \in \ell_2} \frac{\langle \mathbf{c}^\top \mathbf{D}\Psi, \mathbf{d}^\top \mathbf{D}^{-1}\tilde{\Psi}\rangle_{\mathscr{H}}}{\|\mathbf{d}^\top \mathbf{D}^{-1}\tilde{\Psi}\|_{\tilde{\mathscr{V}}^{-s}}} = \sup_{0\neq \mathbf{d}\in\ell_2} \frac{\langle \mathbf{c}, \mathbf{d}\rangle}{\|\mathbf{d}\|} \frac{\|\mathbf{d}\|}{\|\mathbf{d}^\top \mathbf{D}^{-1}\tilde{\Psi}\|_{\tilde{\mathscr{V}}^{-s}}}$, where $\mathbf{D}$ is an invertible diagonal matrix, $\Psi = \cup_j \Psi_j$, and $\tilde{\Psi} = \cup_j \tilde{\Psi}_j$, and the analogous result with interchanged roles of $(\Psi, \mathbf{D})$ and

$(\tilde{\Psi}, \mathbf{D}^{-1})$, one infers that $\kappa_{\mathscr{V}^s}(\mathbf{D}\Psi_j) = \kappa_{\tilde{\mathscr{V}}^{-s}}(\mathbf{D}^{-1}\tilde{\Psi})$, and so in particular that $\kappa_{\mathscr{V}^s}(\bigcup_{j=0}^\infty \rho^{-js}\Psi_j) = \kappa_{\tilde{\mathscr{V}}^{-s}}(\bigcup_{j=0}^\infty \rho^{js}\tilde{\Psi}_j)$.

Remark 2.6 (dual wavelets cont'd). An explicit expression for $\tilde{\Psi}_j$ can be obtained in the following special case: For $j \geq 0$, let Φ_j and $\tilde{\Phi}_j$ be $\mathscr{H}$-biorthogonal Riesz bases for V_j and $\tilde{V}_j$, respectively. Let $\mathbf{M}_j = [\mathbf{M}_{j,0}\,\mathbf{M}_{j,1}]$ be the basis transformation from $\Phi_j \cup \Psi_{j+1}$ to Φ_{j+1}, i.e., $[\Phi_j^\top\, \Psi_{j+1}^\top] = \Phi_{j+1}^\top \mathbf{M}_j$. Analogously, let $[\tilde{\Phi}_j^\top\, \tilde{\Psi}_{j+1}^\top] = \tilde{\Phi}_{j+1}^\top \tilde{\mathbf{M}}_j$. Biorthogonality shows that $\mathbf{M}_{j,0} = \langle \tilde{\Phi}_{j+1}, \Phi_j\rangle_{\mathscr{H}}$, $\mathbf{M}_{j,1} = \langle \tilde{\Phi}_{j+1}, \Psi_{j+1}\rangle_{\mathscr{H}}$, and analogous relations at the dual side, as well as $\tilde{\mathbf{M}}_j = \mathbf{M}_j^{-\top}$.

Now let Ψ_j be constructed as in Prop. 2.4 for the case that $\Theta_j = \Phi_j$ and thus $\operatorname{span}\Theta_j = V_j$. Then (2.4) reads as $\mathbf{M}_{j,1} = (\mathrm{Id} - \mathbf{M}_{j,0}\tilde{\mathbf{M}}_{j,0}^\top)\mathbf{R}_{j,1}$, where $\mathbf{R}_{j,1} = \langle \tilde{\Phi}_{j+1}, \Xi_{j+1}\rangle_{\mathscr{H}}$. We conclude that

$$\mathbf{M}_j = [\mathbf{M}_{j,0}\ \mathbf{R}_{j,1}]\begin{bmatrix}\mathrm{Id} & -\tilde{\mathbf{M}}_{j,0}^\top \mathbf{R}_{j,1}\\ 0 & \mathrm{Id}\end{bmatrix},\ \text{i.e.}\ \tilde{\mathbf{M}}_j = \begin{bmatrix}\mathrm{Id} & 0\\ \mathbf{R}_{j,1}^\top \tilde{\mathbf{M}}_{j,0} & \mathrm{Id}\end{bmatrix}[\mathbf{M}_{j,0}\ \mathbf{R}_{j,1}]^{-\top},$$

meaning that dual wavelets become explicitly available in terms of $\tilde{\Phi}_{j+1}$ when additionally Ξ_{j+1} is chosen such that the basis transformation $[\mathbf{M}_{j,0}\ \mathbf{R}_{j,1}]^{-1}$ from Φ_{j+1} to the two-level basis $\Phi_j \cup \Xi_{j+1}$ is explicitly available.

Classical 'stationary' wavelet constructions on the line provide explicitly given (primal and) dual wavelets. Explicit knowledge of dual wavelets is crucial for applications as data compression and data analysis. For applications as preconditioning and the (adaptive) solving of operator equations, however, dual wavelets do not enter the computation, and wavelet constructions on general, non-rectangular domains usually do not provide them (an exception is [Ste03]). Allowing $\operatorname{span}\Theta_j \neq V_j$, thus giving up explicit knowledge of dual wavelets, gives an enormous additional freedom in the construction of Ψ_{j+1} in Prop. 2.4, which we will also exploit in the current work.

3. Construction of quadratic Lagrange finite element wavelets

3.1. **Multi-resolution analyses.** Given a conforming triangulation $\mathcal{T}_0$ of a polygon $\Omega \subset \mathbb{R}^2$, let $(\mathcal{T}_j)_{j\geq 0}$ be the sequence of triangulations where $\mathcal{T}_{j+1}$ is created from $\mathcal{T}_j$ by subdividing each (closed) triangle $T \in \mathcal{T}_j$ into four sub-triangles by connecting the midpoints of the edges of T (*red-refinement*).

For $\Gamma \subset \partial\Omega$ being a union of closed edges of triangles $T \in \mathcal{T}_0$, we define V_j ($\tilde{V}_j$) as the space of continuous piecewise quadratics (linears) w.r.t. $\mathcal{T}_j$ ($\mathcal{T}_{j+1}$) that vanish at Γ. We let $\mathcal{N}(\mathcal{T}_j)$ denote the set of vertices that are not on Γ of $T \in \mathcal{T}_j$.

We take $\mathscr{H} := L_2(\Omega)$, and for some $t \in [1, \frac{3}{2})$, define $\mathscr{V} = \tilde{\mathscr{V}} := H^1_{0,\Gamma}(\Omega) \cap H^t(\Omega)$. With these definitions, the Jackson and Bernstein estimates (2.2)–(2.3) are satisfied with $\rho = 2^t$. After having equipped V_j and $\tilde{V}_j$ with uniform Riesz bases, later in Sect. 3.3, with the aid of Remark 2.2 we will verify also the remaining condition (2.1) of Theorem 2.1. For $|s| \leq 2$, we define

$$\mathscr{X}^s := \big[(H^1_{0,\Gamma}(\Omega)\cap H^2(\Omega))', H^1_{0,\Gamma}(\Omega)\cap H^2(\Omega)\big]_{\frac{s}{4}+\frac{1}{2}} \simeq \begin{cases} H^1_{0,\Gamma}(\Omega)\cap H^s(\Omega) & s\in[1,2],\\ H^s_{0,\Gamma}(\Omega) & s\in(\frac{1}{2},1),\\ [L_2(\Omega), H^1_{0,\Gamma}(\Omega)]_{\frac{1}{2}} & s=\frac{1}{2},\\ H^s(\Omega) & s\in[0,\frac{1}{2}),\\ (\mathscr{X}^{-s})' & s\in[-2,0).\end{cases}$$

Thanks to the *reiteration theorem* we have that $\mathscr{V}^s \simeq \mathscr{X}^{st}$. Since $t \in [1, \frac{3}{2})$ was arbitrary, from Corollary 2.3 we conclude that if Ψ_j is a uniform $L_2(\Omega)$-Riesz basis for $V_j \cap \tilde{V}_{j-1}^{\perp_{L_2(\Omega)}}$, then for $|s| < \frac{3}{2}$,

$$\bigcup_{j=0}^{\infty} 2^{-js}\Psi_j \text{ is a Riesz basis for } \mathscr{X}^s.$$

From the approximation properties of $(V_j)_j$, we infer that for $j \geq 0$, $\psi_{j+1,x} \in \Psi_{j+1}$, $p \in [1, \infty]$ and $\frac{1}{p} + \frac{1}{q} = 1$,

$$\begin{aligned}|\langle u, \psi_{j+1,x}\rangle_{L_2(\Omega)}| &\leq \|\psi_{j+1,x}\|_{L_p(\Omega)} \inf_{v_j \in V_j} \|u - v_j\|_{L_q(\operatorname{supp}\psi_{j+1,x})} \\ &\lesssim \|\psi_{j+1,x}\|_{L_p(\Omega)}(2^{-j})^2 |u|_{W_q^2(\operatorname{conv\,hull}(\operatorname{supp}\psi_{j+1,x}))} \quad (u \in W_q^2(\Omega) \cap H_{0,\Gamma}^1(\Omega)),\end{aligned}$$

that is, the wavelets will have *cancellation properties of order* 2. In particular, when $\operatorname{conv\,hull}(\operatorname{supp}\psi_{j+1,x}) \cap \Gamma = \emptyset$, $\psi_{j+1,x}$ has 2 *vanishing moments*.

3.2. **Local-to-global basis construction.** Following [DS99c, NS09], in this subsection it will be shown how to reduce the construction of the various collections of functions on Ω, that are needed for the construction of the biorthogonal wavelet basis corresponding to the primal and dual multi-resolution analyses $(V_j)_j$ and $(\tilde{V}_j)_j$, to the construction of corresponding collections of 'local' functions on the reference triangle

$$\boldsymbol{T} = \{\lambda \in \mathbb{R}^3 \colon \sum_{i=1}^{3} \lambda_i = 1, \lambda_i \geq 0\}.$$

For $1 \leq i \leq 3$, let $\boldsymbol{T}_i = \{\lambda \in \boldsymbol{T} \colon \lambda_i \leq \frac{1}{2}\}$, and let $\boldsymbol{T}_4 = \overline{\boldsymbol{T} \setminus \cup_{i=1}^3 \boldsymbol{T}_i}$ (*red-refinement*).

For any closed triangle T, let $\lambda_T(x) \in \boldsymbol{T}$ denote the barycentric coordinates of $x \in T$ with respect to the set of vertices of T ordered in some way.

We consider finite collections of functions $\boldsymbol{\Sigma} = \{\boldsymbol{\sigma}_\lambda : \lambda \in \boldsymbol{I}_{\boldsymbol{\Sigma}}\}$ on $\boldsymbol{T}$, where $\boldsymbol{I}_{\boldsymbol{\Sigma}}$ is a finite set of points in $\boldsymbol{T}$, that satisfy

($\mathcal{V}$) $\boldsymbol{\sigma}_\lambda$ vanishes on any edge or vertex that does not include λ,
($\mathcal{S}$) $\pi(\boldsymbol{I}_{\boldsymbol{\Sigma}}) = \boldsymbol{I}_{\boldsymbol{\Sigma}}$ and $\boldsymbol{\sigma}_\lambda = \boldsymbol{\sigma}_{\pi(\lambda)} \circ \pi$ for any permutation $\pi : \mathbb{R}^3 \to \mathbb{R}^3$,
($\mathcal{I}$) $\boldsymbol{\Sigma}$ is a linearly independent collection of continuous functions.

Such collections of local functions can be used to assemble collections of global functions in a way known from finite element methods: For $j \geq 0$ and with

$$I_{\Sigma_j} := \{x \in \bar{\Omega} \setminus \Gamma : \lambda_T(x) \in \boldsymbol{I}_{\boldsymbol{\Sigma}} \text{ for some } T \in \mathcal{T}_j\}, \tag{3.1}$$

we define the collection $\Sigma_j = \{\sigma_{j,x} \colon x \in I_{\Sigma_j}\}$ of functions on Ω by

$$\sigma_{j,x}(y) = \begin{cases} \mu(x; \mathcal{T}_j)\boldsymbol{\sigma}_{\lambda_T(x)}(\lambda_T(y)) & \text{if } x, y \in T \in \mathcal{T}_j \\ 0 & \text{otherwise} \end{cases} \tag{3.2}$$

with scaling factor $\mu(x; \mathcal{T}_j) := \big(\sum_{\{T \in \mathcal{T}_j \,:\, T \ni x\}} \operatorname{vol}(T)\big)^{-\frac{1}{2}}$. Note that the assumptions ($\mathcal{V}$), ($\mathcal{S}$) and ($\mathcal{I}$) show that Σ_j are linearly independent collections of well-defined, continuous functions on Ω.

Lemma 3.1. *Let $\boldsymbol{\Sigma}$ and $\tilde{\boldsymbol{\Sigma}}$ be two collections of 'local' functions on $\boldsymbol{T}$ both satisfying ($\mathcal{V}$), ($\mathcal{S}$) and ($\mathcal{I}$). Let Σ_j and $\tilde{\Sigma}_j$ denote the corresponding collections of 'global' functions on Ω. Then:*

(i) $\|\langle \Sigma_j, \Sigma_j\rangle_{L_2(\Omega)}\| \leq \big\|\frac{\langle \boldsymbol{\Sigma}, \boldsymbol{\Sigma}\rangle_{L_2(\boldsymbol{T})}}{\operatorname{vol}(\boldsymbol{T})}\big\|$, $\quad \|\langle \Sigma_j, \Sigma_j\rangle_{L_2(\Omega)}^{-1}\| \leq \Big\|\Big(\frac{\langle \boldsymbol{\Sigma}, \boldsymbol{\Sigma}\rangle_{L_2(\boldsymbol{T})}}{\operatorname{vol}(\boldsymbol{T})}\Big)^{-1}\Big\|$.

(ii) *If* $\boldsymbol{I}_{\boldsymbol{\Sigma}} = \boldsymbol{I}_{\tilde{\boldsymbol{\Sigma}}}$, *and* $\mu\mathrm{Id} \leq \frac{\langle \boldsymbol{\Sigma}, \tilde{\boldsymbol{\Sigma}}\rangle_{L_2(\boldsymbol{T})}}{\mathrm{vol}(\boldsymbol{T})} \leq M\mathrm{Id}$ *then* $\mu\mathrm{Id} \leq \langle \Sigma_j, \tilde{\Sigma}_j\rangle_{L_2(\Omega)} \leq M\mathrm{Id}$.

(iii) $$\sup_{\substack{0\neq v_j \in \operatorname{span}\Sigma_j\\ 0\neq \tilde{v}_j\in\operatorname{span}\tilde{\Sigma}_j}} \frac{\langle v_j, \tilde{v}_j\rangle_{L_2(\Omega)}}{\|v_j\|_{L_2(\Omega)}\|\tilde{v}_j\|_{L_2(\Omega)}} \leq \sup_{\substack{0\neq v \in \operatorname{span}\boldsymbol{\Sigma}\\ 0\neq \tilde{v}\in\operatorname{span}\tilde{\boldsymbol{\Sigma}}}} \frac{\langle v, \tilde{v}\rangle_{L_2(\boldsymbol{\Sigma})}}{\|v\|_{L_2(\boldsymbol{\Sigma})}\|\tilde{v}\|_{L_2(\boldsymbol{\Sigma})}}.$$

Proof. We note that for $\tilde{\mathbf{c}}_j \in \ell_2(I_{\tilde{\Sigma}_j})$, $\mathbf{c}_j \in \ell_2(I_{\Sigma_j})$, it holds that

$$\begin{aligned}
&\big\langle \langle \Sigma_j, \tilde{\Sigma}_j\rangle_{L_2(\Omega)}\tilde{\mathbf{c}}_j, \mathbf{c}_j\big\rangle = \langle \mathbf{c}_j^\top \Sigma_j, \tilde{\mathbf{c}}_j^\top \tilde{\Sigma}_j\rangle_{L_2(\Omega)}\\
&= \sum_{T\in\mathcal{T}_j} \frac{\mathrm{vol}(T)}{\mathrm{vol}(\boldsymbol{T})}\Big\langle \sum_{x\in I_{\Sigma_j}\cap T} c_{j,x}\mu(x;\mathcal{T}_j)\boldsymbol{\sigma}_{\lambda_T(x)}, \sum_{y\in I_{\tilde{\Sigma}_j}\cap T} \tilde{c}_{j,y}\mu(y;\mathcal{T}_j)\tilde{\boldsymbol{\sigma}}_{\lambda_T(y)}\Big\rangle_{L_2(\boldsymbol{T})}\\
&= \sum_{T\in\mathcal{T}_j}\Big\langle \frac{\langle \boldsymbol{\Sigma}, \tilde{\boldsymbol{\Sigma}}\rangle_{L_2(\boldsymbol{T})}}{\mathrm{vol}(\boldsymbol{T})}\tilde{\mathbf{c}}_{\mathcal{T}_j,T}, \mathbf{c}_{\mathcal{T}_j,T}\Big\rangle,
\end{aligned}$$

where

$$\begin{aligned}
\tilde{\mathbf{c}}_{\mathcal{T}_j,T} &:= \Big(\tilde{c}_{j,\lambda_T^{-1}(\lambda)}\mu(\lambda_T^{-1}(\lambda);\mathcal{T}_j)\sqrt{\mathrm{vol}(T)}\Big)_{\lambda\in\boldsymbol{I}_{\tilde{\boldsymbol{\Sigma}}}},\\
\mathbf{c}_{\mathcal{T}_j,T} &:= \Big(c_{j,\lambda_T^{-1}(\lambda)}\mu(\lambda_T^{-1}(\lambda);\mathcal{T}_j)\sqrt{\mathrm{vol}(T)}\Big)_{\lambda\in\boldsymbol{I}_{\boldsymbol{\Sigma}}}
\end{aligned}$$

and

$$\begin{aligned}
\sum_{T\in\mathcal{T}_j}\|\tilde{\mathbf{c}}_{\mathcal{T}_j,T}\|^2 &= \sum_{T\in\mathcal{T}_j}\sum_{y\in I_{\tilde{\Sigma}_j}\cap T}|\tilde{c}_{j,y}|^2\mu(y;\mathcal{T}_j)^2\,\mathrm{vol}(T)\\
&= \sum_{y\in I_{\tilde{\Sigma}_j}}|\tilde{c}_{j,y}|^2\mu(y;\mathcal{T}_j)^2\sum_{\{T\in\mathcal{T}_j\,:\,T\ni y\}}\mathrm{vol}(T) = \|\tilde{\mathbf{c}}_j\|^2,
\end{aligned}$$

and similarly $\sum_{T\in\mathcal{T}_j}\|\mathbf{c}_{\mathcal{T}_j,T}\|^2 = \|\mathbf{c}_j\|^2$.

These relations show (ii) and (i), for the latter using that for $A = A^\top > 0$, $\|A\| = \sup_{0\neq x}\frac{\langle Ax,x\rangle}{\|x\|^2}$, $\|A^{-1}\|^{-1} = \inf_{0\neq x}\frac{\langle Ax,x\rangle}{\|x\|^2}$.

Denoting the value of the supremum at the right hand side of (iii) as Q, we have

$$\begin{aligned}
\langle v_j, \tilde{v}_j\rangle_{L_2(\Omega)} &= \sum_{T\in\mathcal{T}_j}\frac{\mathrm{vol}(T)}{\mathrm{vol}(\boldsymbol{T})}\langle v_j\circ\lambda_T^{-1}, \tilde{v}_j\circ\lambda_T^{-1}\rangle_{L_2(\boldsymbol{T})}\\
&\leq Q\sum_{T\in\mathcal{T}_j}\frac{\mathrm{vol}(T)}{\mathrm{vol}(\boldsymbol{T})}\|v_j\circ\lambda_T^{-1}\|_{L_2(\boldsymbol{T})}\|\tilde{v}_j\circ\lambda_T^{-1}\|_{L_2(\boldsymbol{T})}\\
&\leq Q\Big[\sum_{T\in\mathcal{T}_j}\frac{\mathrm{vol}(T)}{\mathrm{vol}(\boldsymbol{T})}\|v_j\circ\lambda_T^{-1}\|^2_{L_2(\boldsymbol{T})}\Big]^{\frac{1}{2}}\Big[\sum_{T\in\mathcal{T}_j}\frac{\mathrm{vol}(T)}{\mathrm{vol}(\boldsymbol{T})}\|\tilde{v}_j\circ\lambda_T^{-1}\|^2_{L_2(\boldsymbol{T})}\Big]^{\frac{1}{2}}\\
&= Q\|v_j\|_{L_2(\Omega)}\|\tilde{v}_j\|_{L_2(\Omega)},
\end{aligned}$$

which completes the proof. □

3.3. **Verification of the uniform inf-sup conditions for** $(V_j, \tilde{V}_j)_{j\geq 0}$**.** As a first application of the local-to-global basis construction discussed in the previous subsection, we will verify the existence of the uniform bounded biorthogonal projectors from (2.1).

Setting $\boldsymbol{I}_0 := \mathbb{N}_0^3 \cap \boldsymbol{T}$, and for $i \geq 1$, $\boldsymbol{I}_i := (2^{-i}\mathbb{N}_0^3 \cap \boldsymbol{T}) \setminus \boldsymbol{I}_{i-1}$, we let $\boldsymbol{N} := \{n_\lambda \colon \lambda \in \boldsymbol{I}_0 \cup \boldsymbol{I}_1\}$ and $\tilde{\boldsymbol{N}} := \{\tilde{n}_\lambda \colon \lambda \in \boldsymbol{I}_0 \cup \boldsymbol{I}_1\}$ denote the standard nodal bases of $P_2(\boldsymbol{T})$ and $C(\boldsymbol{T}) \cap \prod_{i=1}^4 P_1(\boldsymbol{T}_i)$, respectively.

The with $\boldsymbol{N}$ and $\tilde{\boldsymbol{N}}$ corresponding 'global' collections N_j and $\tilde{N}_j$, defined by (3.1)–(3.2), span the spaces V_j and $\tilde{V}_j$, respectively. The index sets of these collections satisfy $I_{N_j} = I_{\tilde{N}_j} = \mathcal{N}(\mathcal{T}_{j+1})$. Lemma 3.1(i) shows that N_j and $\tilde{N}_j$ are uniform $L_2(\Omega)$-Riesz bases for their spans. With $\boldsymbol{I}_0 \cup \boldsymbol{I}_1$ (and $\boldsymbol{I}_2$) numbered as indicated in Figure 1, a direct computation shows that

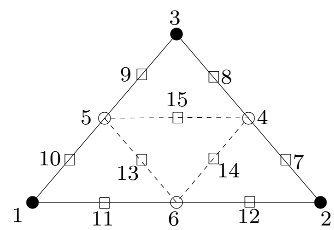

FIGURE 1. Numbering of $\boldsymbol{I}_0 \cup \boldsymbol{I}_1 \cup \boldsymbol{I}_2$.

$$\frac{\langle \boldsymbol{N}, \tilde{\boldsymbol{N}} \rangle_{L_2(\boldsymbol{T})}}{\operatorname{vol}(\boldsymbol{T})} = \frac{1}{480} \begin{bmatrix} 16 & -3 & -3 & -10 & 0 & 0 \\ -3 & 16 & -3 & 0 & -10 & 0 \\ -3 & -3 & 16 & 0 & 0 & -10 \\ 2 & 14 & 14 & 70 & 30 & 30 \\ 14 & 2 & 14 & 30 & 70 & 30 \\ 14 & 14 & 2 & 30 & 30 & 70 \end{bmatrix}.$$

With $\lambda := \lambda_{\min}\big(\frac{1}{2\operatorname{vol}(\boldsymbol{T})}(\langle \boldsymbol{N}, \tilde{\boldsymbol{N}} \rangle_{L_2(\boldsymbol{T})} + \langle \boldsymbol{N}, \tilde{\boldsymbol{N}} \rangle_{L_2(\boldsymbol{T})}^\top)\big) \approx 0.0191$, it holds that $\frac{\langle \boldsymbol{N}, \tilde{\boldsymbol{N}} \rangle_{L_2(\boldsymbol{T})}}{\operatorname{vol}(\boldsymbol{T})} \geq \lambda \mathrm{Id}$ and thus, by Lemma 3.1(ii), $\langle N_j, \tilde{N}_j \rangle_{L_2(\Omega)} \geq \lambda \mathrm{Id}$, which shows that $\sup_j \|\langle N_j, \tilde{N}_j \rangle_{L_2(\Omega)}^{-1}\| \leq \lambda^{-1}$. Now Remark 2.2 shows that the inf-sup condition (1), and thus equivalently (2.1), are indeed satisfied.

3.4. **Local collections $\boldsymbol{\Theta}$, $\boldsymbol{\Xi}$, and $\tilde{\boldsymbol{\Phi}}$ underlying the construction of Ψ_{j+1}.** In order to construct Ψ_{j+1} for $j \geq 0$ by means of equation (2.4), we need to specify the collections Θ_j, Ξ_{j+1} and $\tilde{\Phi}_j$ of functions on Ω. We will construct them from collections $\boldsymbol{\Theta} = \{\boldsymbol{\theta}_\lambda \colon \lambda \in \boldsymbol{I}_0 \cup \boldsymbol{I}_1\}$, $\boldsymbol{\Xi} = \{\boldsymbol{\xi}_\lambda \colon \lambda \in \boldsymbol{I}_2\}$, and $\tilde{\boldsymbol{\Phi}} = \{\tilde{\boldsymbol{\phi}}_\lambda \colon \lambda \in \boldsymbol{I}_0 \cup \boldsymbol{I}_1\}$, respectively, of functions on $\boldsymbol{T}$ that satisfy $(\mathcal{V})$, $(\mathcal{S})$, and $(\mathcal{I})$, and for which $\boldsymbol{\Theta} \cup \boldsymbol{\Sigma}$ and $\tilde{\boldsymbol{\Phi}}$ are bases for $C(\boldsymbol{T}) \cap \prod_{i=1}^4 P_2(\boldsymbol{T}_i)$ and $C(\boldsymbol{T}) \cap \prod_{i=1}^4 P_1(\boldsymbol{T}_i)$, respectively, and $\langle \boldsymbol{\Theta}, \tilde{\boldsymbol{\Phi}} \rangle_{L_2(\boldsymbol{T})} = \operatorname{vol}(\boldsymbol{T})\mathrm{Id}$. Then by an application of Lemma 3.1, we know that, as required, $\Theta_j \cup \Sigma_{j+1}$ and $\tilde{\Phi}_j$ are uniform Riesz bases for V_{j+1} and $\tilde{V}_j$, respectively, and $\langle \Theta_j, \tilde{\Phi}_j \rangle_{L_2(\Omega)} = \mathrm{Id}$. The index sets of these collections satisfy $I_{\Theta_j} = I_{\tilde{\Phi}_j} = \mathcal{N}(\mathcal{T}_{j+1})$, and $I_{\Sigma_{j+1}} = \mathcal{N}(\mathcal{T}_{j+2}) \setminus \mathcal{N}(\mathcal{T}_{j+1})$.

We will specify $\boldsymbol{\Theta} \cup \boldsymbol{\Sigma}$ and $\tilde{\boldsymbol{\Phi}}$ in terms of the usual nodal bases $\boldsymbol{N}_f$ and $\tilde{\boldsymbol{N}}$ for $C(\boldsymbol{T}) \cap \prod_{i=1}^4 P_2(\boldsymbol{T}_i)$ and $C(\boldsymbol{T}) \cap \prod_{i=1}^4 P_1(\boldsymbol{T}_i)$, respectively. For completeness, with $\boldsymbol{N}_f$ we mean the collection of functions in $C(\boldsymbol{T}) \cap \prod_{i=1}^4 P_2(\boldsymbol{T}_i)$ that have value 1 in one of the points of $\boldsymbol{I}_0 \cup \boldsymbol{I}_1 \cup \boldsymbol{I}_2$ and vanish at the others. Aiming at wavelets that have relatively small supports, we exploit the available freedom in the construction to obtain $\boldsymbol{\theta}_\lambda$ and $\boldsymbol{\xi}_\lambda$ with small supports and a matrix $\langle \boldsymbol{\Xi}, \tilde{\boldsymbol{\Phi}} \rangle_{L_2(\boldsymbol{T})}$ that is sparsely populated.

We define $\tilde{\boldsymbol{\Phi}}$ as indicated in Figure 2, and $\boldsymbol{\Theta}$ as indicated in Figure 3. Both these collections satisfy ($\mathcal{V}$), ($\mathcal{S}$), and ($\mathcal{I}$), and $\tilde{\boldsymbol{\Phi}}$ is a basis for $C(\boldsymbol{T}) \cap \prod_{i=1}^{4} P_1(\boldsymbol{T}_i)$. A

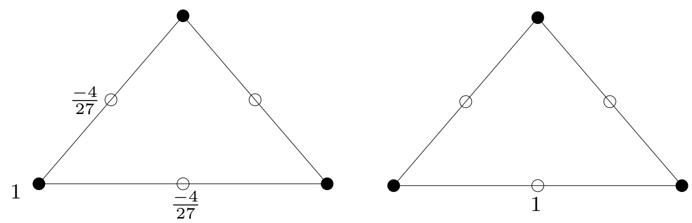

FIGURE 2. $\tilde{\boldsymbol{\phi}}_{(1,0,0)}$ (left) and $\tilde{\boldsymbol{\phi}}_{(\frac{1}{2},\frac{1}{2},0)}$ (right) in terms of $\tilde{\boldsymbol{N}}$. The other $\tilde{\boldsymbol{\phi}}_\lambda$ are obtained by permuting the barycentric coordinates.

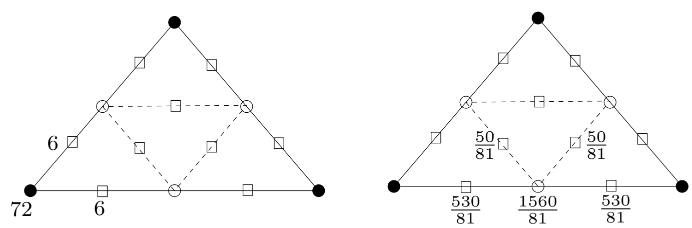

FIGURE 3. $\boldsymbol{\theta}_{(1,0,0)}$ (left) and $\boldsymbol{\theta}_{(\frac{1}{2},\frac{1}{2},0)}$ (right) in terms of $\boldsymbol{N}_f$. The other $\boldsymbol{\theta}_\lambda$ are obtained by permuting the barycentric coordinates.

direct computation shows that $\langle \boldsymbol{\Theta}, \tilde{\boldsymbol{\Phi}} \rangle_{L_2(\boldsymbol{T})} = \mathrm{vol}(\boldsymbol{T})\mathrm{Id}$. We define $\boldsymbol{\Xi}$ as indicated in Figure 4. It satisfies ($\mathcal{V}$), ($\mathcal{S}$), and ($\mathcal{I}$), and since

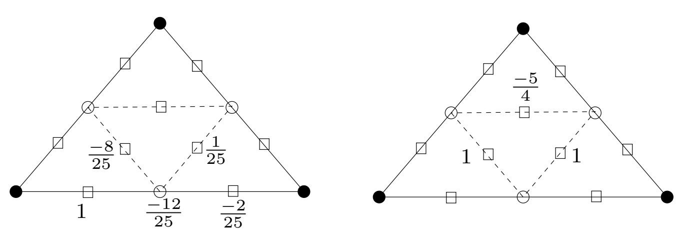

FIGURE 4. $\boldsymbol{\xi}_{(\frac{3}{4},\frac{1}{4},0)}$ (left) and $\boldsymbol{\xi}_{(\frac{1}{4},\frac{1}{4},\frac{1}{2})}$ (right) in terms of $\boldsymbol{N}_f$. The other $\boldsymbol{\xi}_\lambda$'s (five and two) are obtained by permuting the barycentric coordinates.

$$
\begin{vmatrix}
72 & 0 & 0 & 0 & 0 & 0 & 0 & 0 & 0 & 0 & 0 & 0 & 0 & 0 & 0 \\
0 & 72 & 0 & 0 & 0 & 0 & 0 & 0 & 0 & 0 & 0 & 0 & 0 & 0 & 0 \\
0 & 0 & 72 & 0 & 0 & 0 & 0 & 0 & 0 & 0 & 0 & 0 & 0 & 0 & 0 \\
0 & 0 & 0 & \frac{1560}{81} & 0 & 0 & \frac{-12}{25} & \frac{-12}{25} & 0 & 0 & 0 & 0 & 0 & 0 & 0 \\
0 & 0 & 0 & 0 & \frac{1560}{81} & 0 & 0 & 0 & \frac{-12}{25} & \frac{-12}{25} & 0 & 0 & 0 & 0 & 0 \\
0 & 0 & 0 & 0 & 0 & \frac{1560}{81} & 0 & 0 & 0 & 0 & \frac{-12}{25} & \frac{-12}{25} & 0 & 0 & 0 \\
0 & 6 & 0 & \frac{530}{81} & 0 & 0 & 1 & \frac{-2}{25} & 0 & 0 & 0 & 0 & 0 & 0 & 0 \\
0 & 0 & 6 & \frac{530}{81} & 0 & 0 & \frac{-2}{25} & 1 & 0 & 0 & 0 & 0 & 0 & 0 & 0 \\
0 & 0 & 6 & 0 & \frac{530}{81} & 0 & 0 & 0 & 1 & \frac{-2}{25} & 0 & 0 & 0 & 0 & 0 \\
6 & 0 & 0 & 0 & \frac{530}{81} & 0 & 0 & 0 & \frac{-2}{25} & 1 & 0 & 0 & 0 & 0 & 0 \\
6 & 0 & 0 & 0 & 0 & \frac{530}{81} & 0 & 0 & 0 & 0 & 1 & \frac{-2}{25} & 0 & 0 & 0 \\
0 & 6 & 0 & 0 & 0 & \frac{530}{81} & 0 & 0 & 0 & 0 & \frac{-2}{25} & 1 & 0 & 0 & 0 \\
0 & 0 & 0 & 0 & \frac{50}{81} & \frac{50}{81} & 0 & 0 & \frac{1}{25} & \frac{-8}{25} & \frac{-8}{25} & \frac{1}{25} & \frac{-5}{4} & 1 & 1 \\
0 & 0 & 0 & \frac{50}{81} & 0 & \frac{50}{81} & \frac{-8}{25} & \frac{1}{25} & 0 & 0 & \frac{1}{25} & \frac{-8}{25} & 1 & \frac{-5}{4} & 1 \\
0 & 0 & 0 & \frac{50}{81} & \frac{50}{81} & 0 & \frac{1}{25} & \frac{-8}{25} & \frac{-8}{25} & \frac{1}{25} & 0 & 0 & 1 & 1 & \frac{-5}{4}
\end{vmatrix} \neq 0,
$$

we conclude that $\mathbf{\Theta} \cup \mathbf{\Xi}$ is a basis for $C(\boldsymbol{T}) \cap \prod_{i=1}^4 P_2(\boldsymbol{T}_i)$. It holds that

$$
\langle \boldsymbol{\xi}_{(\frac{3}{4},\frac{1}{4},0)}, \tilde{\boldsymbol{\phi}}_\lambda \rangle_{L_2(\boldsymbol{T})} = \mathrm{vol}(\boldsymbol{T}) \times \begin{cases} \frac{3}{100} & \lambda = (1,0,0), \\ 0 & \lambda \in (\boldsymbol{I}_0 \cup \boldsymbol{I}_1) \setminus \{(1,0,0)\}, \end{cases}
$$

$$
\langle \boldsymbol{\xi}_{(\frac{1}{4},\frac{1}{4},\frac{1}{2})}, \tilde{\boldsymbol{\phi}}_\lambda \rangle_{L_2(\boldsymbol{T})} = \mathrm{vol}(\boldsymbol{T}) \times \begin{cases} \frac{-1}{48} & \lambda = (0,0,1), \\ \frac{27}{240} & \lambda = (\frac{1}{2},\frac{1}{2},0), \\ 0 & \lambda \in (\boldsymbol{I}_0 \cup \boldsymbol{I}_1) \setminus \{(0,0,1),(\frac{1}{2},\frac{1}{2},0)\}, \end{cases}
$$

where the other values of $\langle \boldsymbol{\xi}_\mu, \tilde{\boldsymbol{\phi}}_\lambda \rangle_{L_2(\boldsymbol{T})}$ for $(\mu,\lambda) \in \boldsymbol{I}_2 \times (\boldsymbol{I}_1 \cup \boldsymbol{I}_0)$ are obtained by permuting the barycentric coordinates.

3.5. **Definition of the Ψ_j.** We take $\Psi_0 = N_0$, being a Riesz basis for V_0. In the previous subsection, from corresponding local collections we have constructed uniform Riesz bases $\Theta_j \cup \Sigma_{j+1}$ and $\tilde{\Phi}_j$ for V_{j+1} and $\tilde{V}_j$, respectively, such that $\langle \Theta_j, \tilde{\Phi}_j \rangle_{L_2(\Omega)} = \mathrm{Id}$. For $j \geq 0$, the collection of wavelets Ψ_{j+1} is now given by the explicit formula $\Psi_{j+1} = \Xi_{j+1} - \langle \Xi_{j+1}, \tilde{\Phi}_j \rangle_{L_2(\Omega)} \Theta_j$. These wavelets will depend on the topology of $\mathcal{T}_0$ via the the local-to-global basis construction (3.1)–(3.2) that we applied for the definition of Θ_j, Σ_{j+1}, and $\tilde{\Phi}_j$, as well via the inner product $\langle \Xi_{j+1}, \tilde{\Phi}_j \rangle_{L_2(\Omega)}$.

Despite of these dependencies on $\mathcal{T}_0$, as well as that on Γ, we can distinguish between two types of wavelets: A wavelet $\psi_{j+1,x}$ of the first type stems from $\boldsymbol{\xi}_\lambda$ of type $\boldsymbol{\xi}_{(\frac{3}{4},\frac{1}{4},0)}$ (see Figure 4), so that $x \in \mathcal{N}(\mathcal{T}_{j+2}) \setminus \mathcal{N}(\mathcal{T}_{j+1})$ is on an edge of a $T \in \mathcal{T}_j$. It equals $\xi_{j+1,x}$ minus a multiple of *one* (or, near the Dirichlet boundary, possibly zero) $\theta_{j,y}$ with $y \in \mathcal{N}(\mathcal{T}_j)$ (left picture in Figure 2). A wavelet $\psi_{j+1,x}$ of the second type stems from $\boldsymbol{\xi}_\lambda$ of type $\boldsymbol{\xi}_{(\frac{1}{4},\frac{1}{4},\frac{3}{4})}$, so that $x \in \mathcal{N}(\mathcal{T}_{j+2}) \setminus \mathcal{N}(\mathcal{T}_{j+1})$ is interior to a $T \in \mathcal{T}_j$. It equals $\xi_{j+1,x}$ minus a multiple of *two* (or, near the Dirichlet boundary, possibly one or zero) $\theta_{j,y}$'s, where one $y \in \mathcal{N}(\mathcal{T}_j)$ and the other is in $\mathcal{N}(\mathcal{T}_{j+1}) \setminus \mathcal{N}(\mathcal{T}_j)$ (right picture in Figure 2). The supports of both types of wavelets (away from the Dirichlet boundary) are illustrated in Figure 5.

3.6. **Condition numbers.** For $\Omega = (0,1)^2$, $\mathcal{T}_0 = \big\{\{(x,y)\colon 0 \leq x \leq y \leq 1\}, \{(x,y)\colon 0 \leq y \leq x \leq 1\}\big\}$, and $\Gamma = \partial\Omega$, we have computed $\kappa_{L_2(\Omega)}(\bigcup_{j=0}^J \Psi_j)$

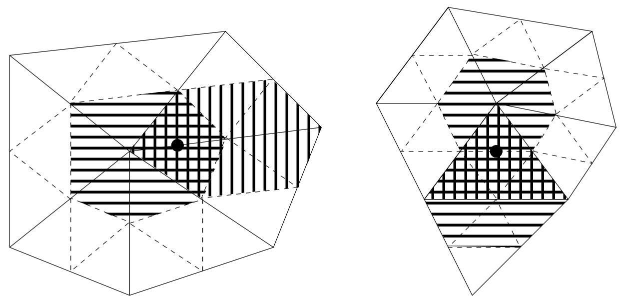

FIGURE 5. Wavelets $\psi_{j+1,x}$ for $x \in \mathcal{N}(\mathcal{T}_{j+2}) \setminus \mathcal{N}(\mathcal{T}_{j+1})$ on an edge of a $T \in \mathcal{T}_j$ (left) or interior to a $T \in \mathcal{T}_j$ (right). Indicated are x ($\bullet$), the support of $\xi_{j+1,x}$ (vertical shading), and that of the $\theta_{j,y}$'s (horizontal shading). The support of the wavelet is the union of these supports.
The wavelets are linear combinations of 11 (left) or 13 (right) quadratic nodal basis functions (i.e. functions from N_{j+1}) (the numbers 11 and 13 apply when the valence of each interior vertex in $\mathcal{T}_j$ is 6).

TABLE 1. L_2-condition numbers of the L_2-normalized wavelets up to level J.

J	0	1	2	3	4	5	6	7	8
$\kappa_{L_2((0,1)^2)}$	1	4.8	7.3	8.3	8.9	9.2	9.7	9.8	9.9

TABLE 2. H_0^1-condition numbers of the H_0^1-normalized wavelets up to level J.

J	0	1	2	3	4	5	6	7	8
$\kappa_{H_0^1((0,1)^2)}$	1	27	41	54	63	70	76	81	85

and $\kappa_{H_0^1(\Omega)}(\bigcup_{j=0}^J \Psi_j)$, with $H_0^1(\Omega)$ equipped with $|\cdot|_{H^1(\Omega)}$, and with the wavelets normalized in the corresponding norm. That is, we have computed the condition numbers of the (normalized) mass and stiffness matrices. The results are given in Tables 1 and 2.

Remark 3.2. The principles behind the finite element wavelet construction applied in this work were introduced in [Ste98a, DS99c]. The realizations of finite element wavelets for given primal and dual orders from [DS99c] were revisited in [NS09] in order to obtain smaller condition numbers. The two-dimensional piecewise quadratic wavelets from [NS09] have 3 vanishing moments (since $\tilde{V}_j = V_j$). Their L_2- and H_0^1-condition numbers on the square on level $J = 6$ were 12 and 60, respectively, for the H_0^1-case somewhat improving upon the condition numbers from Table 2. On the other hand, for a regular mesh where all vertices have valence 6, each quadratic wavelet away from the boundary in [NS09] is a linear combination of not less than 87 nodal basis functions, which high number was the motivation for the current work.

TABLE 3. H^1-condition numbers of the H^1-normalized *dual* wavelets up to level J.

J	0	1	2	3	4	5	6
$\kappa_{H_0^1((0,1)^2)}$	1	6.5	14	22	28	32	36

Two-dimensional quadratic finite element wavelets where each wavelet is a linear combination of only 4 or 6 nodal basis functions were introduced in [Liu06]. These wavelets are based on a splitting of V_{j+1} into V_j and an orthogonal complement w.r.t. a 'discrete' level-dependent scalar product on V_{j+1}. It was shown that the wavelets generate a Riesz basis for H^s for $s \in (0.3974, \frac{3}{2})$. These wavelets, however, have no vanishing moment, and, consequently, they cannot be expected to generate a Riesz basis for H^s for $s \leq 0$.

Finally, since for our application in solving parabolic PDEs it is needed that the wavelets form a Riesz basis in $H^{-1}(\Omega)$, based on $\kappa_{H^{-1}(\Omega)}(\mathbf{D}\Psi) = \kappa_{H_0^1(\Omega)}(\mathbf{D}^{-1}\tilde{\Psi})$ (see Remark 2.5), where $\tilde{\Psi}$ is the dual wavelet basis, additionally we have computed $\kappa_{H_0^1(\Omega)}(\bigcup_{j=0}^{J} \tilde{\Psi}_j)$ with these dual wavelets being normalized w.r.t. $|\cdot|_{H^1(\Omega)}$. The results are given in Table 3. Since, as explained in Remark 2.6, these computations involve the applications of inverses of mass matrices and that of two-level transforms at the primal side, which inverses in our case are densely populated, we computed these condition numbers only up to level 6.

REFERENCES

[CTU99] C. Canuto, A. Tabacco, and K. Urban. The wavelet element method part I: Construction and analysis. *Appl. Comput. Harmon. Anal.*, 6:1–52, 1999.

[Dah96] W. Dahmen. Stability of multiscale transformations. *J. Fourier Anal. Appl.*, 2(4):341–362, 1996.

[Dah97] W. Dahmen. Wavelet and multiscale methods for operator equations. *Acta Numer.*, 6:55–228, 1997.

[DS99a] W. Dahmen and R. Schneider. Composite wavelet bases for operator equations. *Math. Comp.*, 68:1533–1567, 1999.

[DS99b] W. Dahmen and R. Schneider. Wavelets on manifolds I: Construction and domain decomposition. *SIAM J. Math. Anal.*, 31:184–230, 1999.

[DS99c] W. Dahmen and R.P. Stevenson. Element-by-element construction of wavelets satisfying stability and moment conditions. *SIAM J. Numer. Anal.*, 37(1):319–352, 1999.

[FQ00] M. S. Floater and E. G. Quak. Linear independence and stability of piecewise linear prewavelets on arbitrary triangulations. *SIAM J. Numer. Anal.*, 38(1):58–79, 2000.

[HM00] D. Hong and Y.A. Mu. Construction of prewavelets with minimum support over triangulations. In *Wavelet analysis and multiresolutionFOswa methods,* proceedings Urbana-Champaign, IL, 1999, Lecture Notes in Pure and Appl. Math. 212, pages 145–165, Marcel Dekker, Inc., New York, 2000.

[KO95] U. Kotyczka and P. Oswald. Piecewise linear prewavelets of small support. In C.K. Chui and L.L. Schumaker, editors, *Approximation Theory VIII.* World Scientific Publishing Co. Inc., 1995.

[Liu06] S.-T. Liu. Quadratic stable wavelet bases on general meshes. *Appl. Comput. Harmon. Anal.*, 20(3):313–325, 2006.

[LO96] R. Lorentz and P. Oswald. Multilevel finite element Riesz bases in Sobolev spaces. In P. Bjørstad, M. Espedal, and Keyes D., editors, *Proc. 9th. Symp. on Domain Decomposition Methods.* John Wiley & Sons, 1996.

[NS09] H. Nguyen and R.P. Stevenson. Finite element wavelets with improved quantitative properties. *J. Comput. Appl. Math.*, 230(2):706–727, 2009.

[RS18] N. Rekatsinas and R. Stevenson. Optimal adaptive wavelet methods for first order system least squares: Parabolic problems. Technical report, January 2018.

[Ste98a] R.P. Stevenson. Piecewise linear (pre-)wavelets on non-uniform meshes. In *Multigrid methods V (Stuttgart, 1996)*, volume 3 of *Lect. Notes Comput. Sci. Eng.*, pages 306–319. Springer, Berlin, 1998.

[Ste98b] R.P. Stevenson. Stable three-point wavelet bases on general meshes. *Numer. Math.*, 80:131–158, 1998.

[Ste03] R.P. Stevenson. Locally supported, piecewise polynomial biorthogonal wavelets on non-uniform meshes. *Constr. Approx.*, 19(4):477–508, 2003.

[Ste09] R.P. Stevenson. Adaptive wavelet methods for solving operator equations: An overview. In R.A. DeVore and A. Kunoth, editors, *Multiscale, Nonlinear and Adaptive Approximation: Dedicated to Wolfgang Dahmen on the Occasion of his 60th Birthday*, pages 543–598. Springer, Berlin, 2009.

[Urb09] K. Urban. *Wavelet Methods for Elliptic Partial Differential Equations*. Oxford University Press, 2009.

[VW96] P.S. Vassilevski and J. Wang. Stabilizing the hierarchical basis by approximate wavelets, I: Theory. *Num. Lin. Alg. with Appl.*, 1:1–23, 1996.

Korteweg-de Vries Institute for Mathematics, University of Amsterdam, P.O. Box 94248, 1090 GE Amsterdam, The Netherlands

E-mail address: n.rekatsinas@uva.nl, r.p.stevenson@uva.nl